MULTI-SENSOR CHARACTERIZATION OF MAMMATUS CLOUDS IN EUROPE AND THE U.S.

6B.2

Silke Trömel[1], Alexander V. Ryzhkov[2], Malte Diederich[1], Kai Mühlbauer[1], Clemens Simmer[1], Stefan Kneifel[3]

[1]Meteorological Institute, University of Bonn, Germany

[2]Cooperative Institute for Mesoscale Meteorological Studies, University of Oklahoma, Norman, Oklahoma, and NOAA/OAR/National Severe Storms Laboratory, Norman, Oklahoma

[3] Institute for Geophysics and Meteorology, University of Cologne, Germany

1. INTRODUCTION

On June 6, 2014 (Pentecost), especially the north-western part of Germany (Northrhine Westphalia), was affected by a high precipitation supercell, which also developed into a bow echo. The storm was described as one of the most violent since decades by the German weather service (DWD). During this event six fatalities, devastating wind gusts up to 150km/h, hail and a flash flood in Düsseldorf has been reported. Diederich and Evaristo (2015) generated a national 3D radar composite for this day based on the C band radar network of DWD, recently upgraded to polarimetry, with 1 km horizontal, 250 m vertical and 5 minutes temporal resolution.

First, the aim of the study has been an analysis on the predictive value of so-called Z_{DR}-columns based on this day. Z_{DR}-columns are vertically extended enhancements of differential reflectivity Z_{DR}, detectable e.g. in radar-measured vertical cross sections (RHI scans), or 3D radar composites. They can extend several kilometers above the 0^0C level and indicate supercooled liquid raindrops lofted by intense updrafts. Thus, Z_{DR}-columns in general are considered as polarimetric descriptors for the extent and intensity of updrafts in storms and thus are early signs of rainfall intensification and hail (Picca et al., 2010; Kumjian et al., 2014). Visual inspection of the radar data reveals the existence of pronounced Z_{DR}-columns, e.g. in the genuine RHI measured with the polarimetric X band radar in Bonn, BoXPol, while the bow echo also grazes the city of Bonn (at 18:30 UTC, not shown). Columns of high differential reflectivity in the mature stage are visible protruding the 0°C level at around 3.8 km height. The monitored cross-section also reveals the signatures of a supercell, i.e. the wall, the forward overhang, and the echo-free vault (Browning 1964). The echo-free vault or bounded weak echo region is associated with the primary updraft of a supercell and accordingly one of the Z_{DR}-columns appears closely collocated with the vault.

In addition to these Z_{DR}-columns also mammatus clouds have been identified in the leading anvil of the storm. The RHI measured with BoXPol clearly shows the characteristic appearance of these hanging protuberances. Their occurrence is also confirmed by supplementary measurements available in Bonn and Jülich (both cities are located in the western part of Germany most affected by the storm in about 50km distance to each other) like ceilometers, microwave radiometers, a 36 GHz cloud radar, a 1.5μm Doppler lidar, a total sky imager but also by photographs and videos from laypersons. A short selection only is presented in this paper.

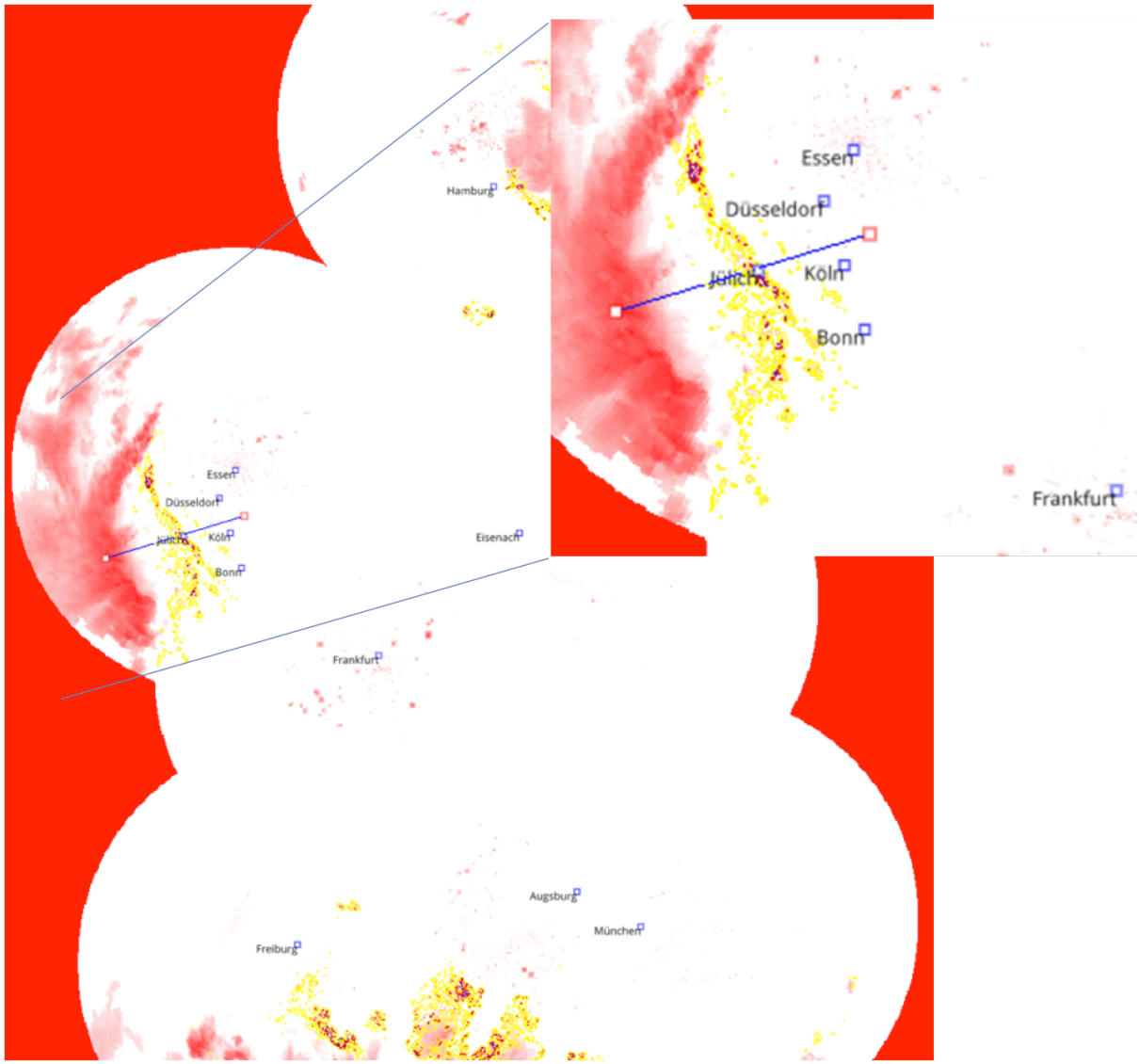

Fig. 1: A snapshot from 9 June 2014 at 17:40 UTC indicating surface reflectivity in shades of red and the Z_{DR}-column product based on the national C band radar composite in yellow and red for values equal to 3 and 7, including an enlarged image of the area of interest. The blue line indicates the position of the vertical cross section through the underlying composite shown in Fig. 2.

It turned out, that these mammatus clouds high above the freezing level in the anvil of the storm not only influenced the envisioned analysis on Z_{DR}-columns but finally changed the direction of our research.

In order to quantify the updraft associated with Z_{DR}-columns, Picca et al. (2010) introduced the so-called Z_{DR}-column product. Assuming the radar volume data is already interpolated on a regular three-dimensional Cartesian (x,y,z) grid, the Z_{DR}-column product counts for each (x,y) coordinate the number of vertical grid boxes above the 0^0C level with Z_{DR} values in excess of a predefined threshold of 1 or 2 dB. However, if we simply count the number of grid boxes aloft with enhanced Z_{DR} in excess of 1dB as outlined in Picca et al. (2010), the results based on the 3D composite are unexpected at first glance. Fig. 1 shows a snapshot of the temporal development of surface reflectivities together with the ‚pseudo-Z_{DR}-column product'. The reddish colors show the surface reflectivity and the yellow, embedded orange, and red colors indicate the contour lines for 3, 5, and 7 grid points with

Z_{DR} greater than 1dB above the 0°C level. A detailed analysis reveals that not all Z_{DR}-signals are related to Z_{DR}-columns and explains the denotation ‚pseudo Z_{DR}-column product':

Even for intense supercells, more often observed in the U.S. than in Germany, lead times grater than 10-20 min between the Z_{DR}-column product and intensification of surface rainfall are unexpected, i.e. have never been observed so far. However, Fig. 1 is a snapshot at 17:40 UTC and the box on the right shows a zoom into our Bonn/Jülich area with enhanced Z_{DR} aloft at remarkable distance of approximately 50km ahead of the storm indicating the storm up to 1 h in advance. On the other hand, a movie reveals these enhanced Z_{DR} values aloft also after the system passed in the trailing anvil and sometimes at the side. Similar to Picca et al. (2010) we used the ratio of pixels with reflectivities Z_H > 40 dBz to the number of pixels with Z_H> 20 dBz below the freezing level as a proxy for heavy precipitation at the surface. Thus, a correlation analysis between the reflectivity pixel ratio $Z_H(40dBz)/Z_H(20dBz)$ and the Z_{DR}-column product for 10km **x**10km boxes for different lag times mostly shows no significant results; only a small fraction of detected updrafts eventually produces meaningful precipitation. Ensuing multi-sensor analyses clearly show that part of the detected updrafts are associated with mammatus clouds high above the freezing level. The microphysical characterization of mammatus clouds based on these multi-sensor observation, however, is partly difficult. In the following section we describe the multi-sensor observations of the anvil associated with mammatus clouds. In section 3 pronounced polarimetric fingerprints observed with high-resolved RHIs from Oklahoma confirm the signatures measured in Germany. Section 4 offers two hypotheses, which may explain the observations presented. Finally, Section 5 summarizes and concludes the analyses.

2. MULTI-SENSOR OBSERVATIONS OF MAMMATUS CLOUDS

The elevated enhanced Z_{DR}-values indicated in Fig. 1 are located at 17:40 UTC directly above Jülich, where the Jülich ObservatorY for Cloud Evolution (JOYCE, Löhnert et al. 2014) with a variety of state-of-the-art remote sensing and in-situ instruments is located. Additionally, a new Python tool allows drawing arbitrary vertical cross sections through the 3D radar composite at any time and any location of the storm. The straight blue line in Fig. 1 indicates the location of the vertical cross section through the composite displayed in Fig. 2. The different panels show horizontal reflectivity Z_H, differential reflectivity Z_{DR}, cross correlation coefficient ρ_{HV} and specific differential phase K_{DP}. We can identify the enhanced Z_{DR} values aloft at the underside of the anvil, which produced the trailing ‚pseudo-Z_{DR}-column product' signal at great distance from the surface reflectivities in the snapshot shown in Fig.1 and during a longer time period during this day. The values are in the range of 2dB between 5 and 8 km height at the underside of the anvil, at first glance suggesting the existence of supercooled liquid drops like in Z_{DR}-columns. Z_{DR} values around 2dB between 5 and 8 km height, however, would correspond to supercooled liquid drops of about 4 mm in diameter at temperatures between -15 and -30°C. Similar cross-sections at the same location approximately 10 minutes before and after show maximal Z_{DR} values in the anvil region between 1.6 dB and 2.5dB. Note, smaller magnitudes of Z_{DR} have been observed in the trailing anvil.

Furthermore, localized updrafts have been detected in the mammatus region with the birdbath scan of BoXPol (not shown) and indirectly are also visible in the cross-section shown in Fig. 2. The polarimetric fingerprint for differential sedimentation consisting amongst others of gradients in Z_H and Z_{DR} showing in the opposite direction is visible at the underside of the anvil. Z_H decreases while Z_{DR} increases towards the base of the anvil and updraft is one possible mechanism causing differential sedimentation or size sorting. In updrafts the smaller drops or lighter hydrometeors are lofted to higher altitudes and are removed from the spectrum, while the bigger drops or heavier hydrometeors remain,

resulting in a decrease in Z_H while Z_{DR} increases.

It can be concluded, that the signatures in Fig.2 do not represent Z_{DR}-columns but the detection algorithm applied revealed in Fig. 1 a mixture of real Z_{DR}-columns and elevated local updrafts in mammatus clouds very high above the freezing levels. The following supplementary measurements clearly demonstrate that these updrafts are associated with mammatus clouds. So, especially for nowcasting applications it is important to be precise with the definition and detection algorithm of Z_{DR}-columns. In order to avoid false designations or better have both, a detection strategy for Z_{DR}-columns and mammatus clouds, it has to be verified whether vertically consecutive grid points above the 0 °C level exceed a certain threshold in Z_{DR} (1 or 2dB) and whether the Z_{DR}-column is not detached from the freezing level. This definition is also used in Snyder et al. (2015).

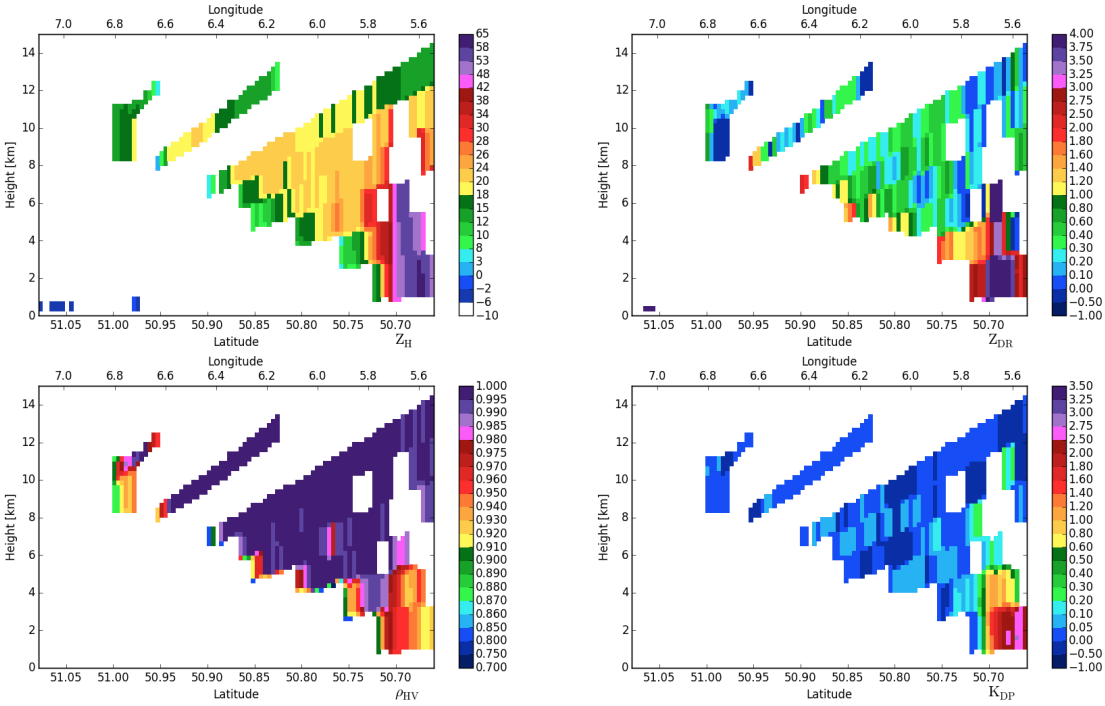

Fig.2: Cross section through the 3D composite along the line indicated in Fig. 1 showing the polarimetric variables Z_H (top left), Z_{DR} (top right), r_{HV} (bottom left), and K_{DP} (bottom right).

Finally, taking these two points into account allows both, detecting and distinguishing between Z_{DR}-columns and elevated local updrafts in mammatus clouds very high above the freezing levels.

Supplementary measurements from JOYCE clearly show that the elevated updrafts high above the freezing level are associated with mammatus clouds (recall Fig. 1, the blue line indicating the location of the cross section shown crosses JOYCE and the pseudo-Z_{DR}-columns / elevated mammatus are directly located above JOYCE during that time). Fig. 3 shows a zoom into the underside of the anvil for more details of the most intense mammatus lobes passing around 17:40 UTC. The different panels show the Doppler spectral width, reflectivity and Doppler velocity measured by the 35.5GHz cloud radar JOYRA-35 while pointing vertically. The

overlaid black and white dots represent the location of a liquid layer as derived from the 1.5μm Doppler lidar.

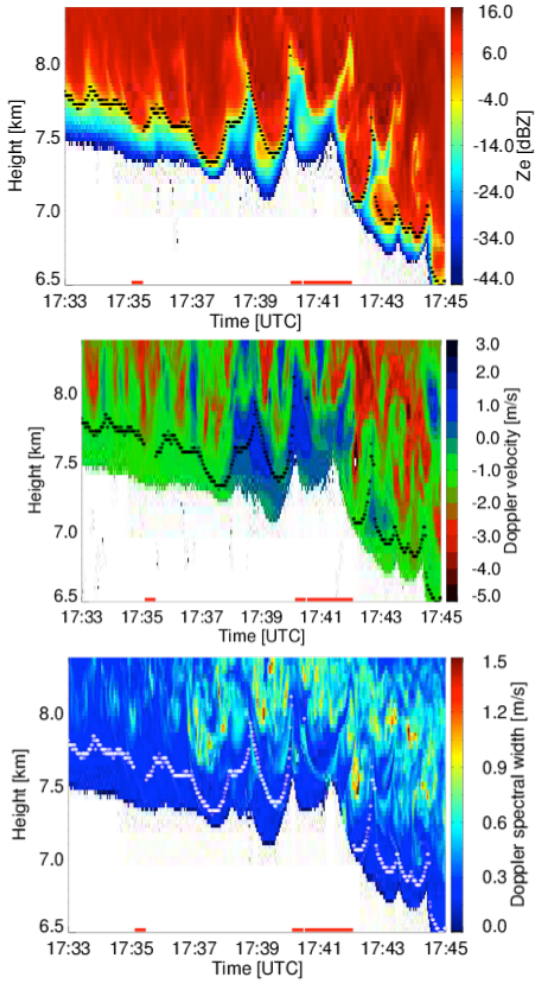

Fig. 3: Detailed zoom in the underside of the anvil with the most intense mammatus lobes. The different panels show effective reflectivity factor (top), Doppler velocity (middle, positive values show updrafts), and spectral width (bottom) measured at JOYCE between 17:39 and 17:45 UTC on 9 June 2014 with the JOYRA-35 cloud radar. Overlaid black and white dots represent the location of a liquid layer as identified with the co-located 1.5μm Doppler lidar measurements.

Unlike for the earlier ice cloud region, the backscattering gradients measured with the Doppler lidar are very sharp (not shown). These sharp gradients represent a clear indication for the presence of supercooled liquid water at these low subfreezing temperatures. Applying a simple signal threshold to the lidar backscattering data, the vertical positions of the liquid water layers (represented by white and black dots, respectively) in Fig. 3 have been derived. The lidar traces the structure of the mammatus clouds in close agreement with the cloud radar. The liquid layer detected by the lidar is found to coincide with the region of largest Ze gradient. In agreement with previous publications on mammatus clouds (Martner 1995; 1996) also a negative correlation between Doppler velocity and reflectivity is visible, i.e. updrafts are associated with smaller reflectivities. The updrafts reach values around 1.5m/s (see middle panel). According to Rauber and Tokay (1991) much weaker updrafts are already sufficient to produce liquid in reasonable amounts for a wide range of drop size distributions. E.g. Rauber and Tokay (1991) estimated that at -22°C updrafts of 0.03m/s are sufficient to produce liquid in reasonable amounts, thus the existence of supercooled water is likely. These drops surely coexist with ice particles but their amount seems to be not sufficient to deplete liquid water generated in these very localized but quite strong updrafts with magnitudes up to 1.5m/s. Additionally, the bottom panel shows enhanced Doppler spectral width around 0.8m/s corresponding to dissipitation rates of about 185cm^2/s^3 collocated with the intense mammatus lobes. Thus, enhanced turbulence has to be expected in the mammatus region.

3. Supporting measurements in Oklahoma

Similar but even more extreme polarimetric signatures have been observed in Oklahoma. Fig. 4 shows a genuine RHI, a high resolution vertical cross-section, measured with the S Band radar in Oklahoma during the tornadic storm on May 29, 2004. Again, like in the observations from Germany we observe remarkably strong and pronounced polarimetric radar signatures along the sloping bases of cumulonimbus anvil clouds

associated with clearly visible mammatus clouds. Z_{DR} exceeds 4 dB, which would correspond to diameters up to 5-6 mm of the largest hypothetically existing supercooled liquid drops at the very bottom of the sloping anvil. Again, Z_H decreases and Z_{DR} rapidly increases towards the bottom of the anvil signaling differential sedimentation of liquid drops or other hydrometeors.

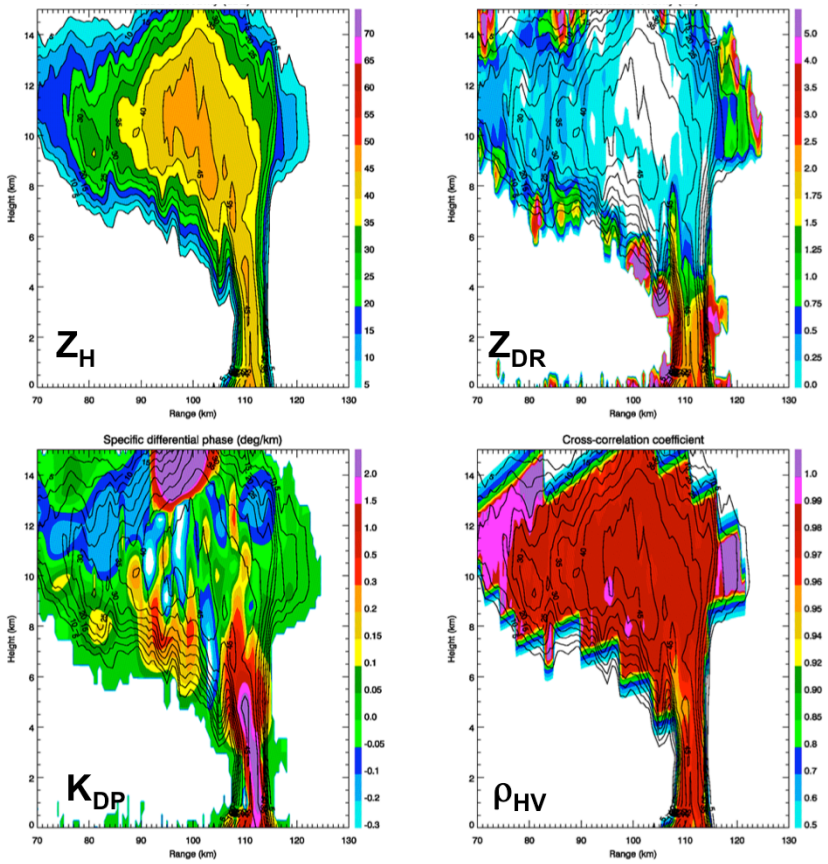

FIg.4: Genuine RHI measured with the S Band radar in Oklahoma during the strong tornadic storm on May 29, 2004.

4. Interpretation of the high Z_{DR}-values in mammatus clouds

The existence of supercooled liquid drops in mammatus clouds at very low subfreezing temperatures as well as the localized updrafts up to 1.5 m/s in magnitude are clearly documented in the observations. Two possible explanations for the origin of these very high Z_{DR}-values - around 2dB for the German case study and 4dB for the Oklahoma case – will be discussed in the following.

Hypothesis 1: Supercooled liquid drops up to 4mm in diameter

Z_{DR}-values around 2dB detected during the Pentecost storm between 5 and 8 km height at the underside of the anvil may suggest supercooled liquid drops of about 4 mm in diameter at temperatures between -15 and -30°C, respectively. Higher Z_{DR}-values observed during the tornadic storm in Oklahoma suggest even largest drops up to 5-6 mm in diameter. In both cases, the hypothesized big drops certainly coexist with ice particles and may be generated in the very localized and strong updrafts. According to Rauber and Tokay (1991) the existence of

supercooled liquid water is possible even at very low subfreezing temperatures in case the amount of ice particles is insufficient to deplete the liquid water generated. First, it appears unlikely that pristine ice crystals at the underside of the anvil produced this high Z_{DR} signal. Ice with higher reflectivity above should fall with higher terminal velocities and is expected to overtake smaller size pristine crystals in their fall. According to Bailey and Hallet (2009), highly anisotropic ice crystals (needles or dendrites) which are able to produce such high Z_{DR} values are especially expected at temperatures around -5°C or -15°C, which deviates considerably from the temperatures range observed during the Pentecost storm at heights with mamma occurrences. On the other hand, updrafts and a lack of ice particles that can absorb the water vapor may lead to significant supersaturation and nucleation of liquid droplets; in such a turbulent environment these droplets could grow rather efficiently into larger drops. Since a collision with ice would result in freezing, very low ice concentrations would be important.
These big drops should also be observable at lower heights. It is quite unlikely that such big drops do not fall out or evaporate completely. Even if the large raindrops freeze quickly, the resulting frozen drops cannot sublimate immediately and they still have very high terminal velocities. Thus, they should be observed at lower height levels but no observational evidence for their existence have been found below the anvil or close to the surface.

An analysis of the Doppler spectra measured by the cloud radar also shows no indication of large drops, which would cause strong bimodality of the spectra since raindrops with 4mm in diameter are expected to have terminal velocities of about 10 m/s at those heights. Instead, most spectra inside the mammatus lobes away from the turbulent regions show a singular peak with typical ice/snow fall velocity of 1 m/s. Within the perimeter of the mammatus rare bimodal spectra can be found with a second smaller peak close to 0 m/s possibly caused by supercooled droplets. These findings in general agree with the supercooled layer indicated by the lidar. The columnar liquid water estimates from the collocated microwave radiometer indicate existence of liquid water inside the cloud, however, with comparably low amounts of less than 100gm^{-2}.

HYPOTHESIS 2: HIGHLY ANISOTROPIC ICE CRYSTALS

The second hypothesis in order to explain the high Z_{DR}-values aloft includes the generation of highly anisoptropic ice crystals. New ice nucleation could occur at the bottom of the anvil due to local updrafts up to 1.5 m/s producing strong supersaturation. The air could be supersaturated with respect to ice and water so that not only new ice but small size cloud droplets can be produced. Note, the existence of supercooled liquid water has been confirmed with simultaneous lidar measurements. This supercooled water can facilitate ice growth. In case of low or zero updrafts, i.e. at the tops of detected updrafts droplets may evaporate and ice crystals may grow at the expense of water vapor according to the Bergeron-Findeisen mechanism.
This locally generated new ice can be anisotropic and has small size and low terminal velocity. Hence, it may be responsible for the high measured Z_{DR}-values but it sublimates almost immediately in a very dry air below the anvil such that no meteorological radar echoes have been detected at lower heights.

5. SUMMARY AND OUTLOOK

Available microphysical observations inside mammatus are inconsistent (Schultz et al. 2006). Hlad (1944) participated in an aircraft flight through mammatus and described them as rain sacks, which must be suspended by strong upward vertical motion. Stith (1995), however, reported regions dominated by aggregated ice particles and negligible liquid water amounts. In general, the temperatures below freezing in most observations makes the existence of an ice component probable, and considerations by Clough and Franks (1991) that sublimation occurs more rapidly and over shorter distances than evaporation also suggests the existence of ice hydrometeors in

mammatus clouds.

We observed pronounced polarimetric radar signatures along the sloping bases of cumulonimbus anvil clouds associated with clearly visible mammatus clouds. Z_H decreases and Z_{DR} rapidly increases towards the bottom of the anvil signaling differential sedimentation of liquid drops at very low subfreezing temperatures (between -15 and -30°C for the German case study). It can be assumed that these supercooled liquid drops are generated in localized updrafts at the underside of the anvil. Maximal observed updrafts reach 1.5m/s. Based on 3D polarimetric radar composites, an automated detection strategy of intense mammatus lobes is possible due to high Z_{DR}-values high above the freezing level in the mammatus region. The detection strategy is similar but especially for nowcasting applications requires a clear distinction from the detection of Z_{DR}-columns. While Z_{DR}-columns are signaling rainfall intensification and hail, the automated detection of updrafts associated with mammatus clouds may be of interest for aviation security due to the associated enhanced turbulence and supercooled liquid water.

The observations of high Z_{DR}-values of around 2dB in the German case study and around 4dB in the tornadic storm in Oklahoma are more likely explainable by highly anisotropic ice crystals generated by the Bergeron-Findeisen process at the tops of the localized updrafts. An alternative explanation of such high Z_{DR}-values with supercooled liquid drops up to 4mm in diameter for the German case study and 5-6mm for the tornadic storm observed in the U.S. are very unlikely, because these drops are not detected at lower heights and also not detectable in the Doppler spectra of the JOYRA-35 cloud radar data.

5. REFERENCES

Bailey, M. P. and J. Hallett, 2009: A Comprehensive Habit Diagram for Atmospheric Ice Crystals: Confirmation from the Laboratory, AIRS II, and Other Field Studies. *J. Atmos. Sci.*, **66**, 2888–2899. Doi: http://dx.doi.org/10.1175/2009JAS2883.1

Browning, K. A., 1964: Airflow and precipitation trajectories within severe local storms which travel to the right of the winds. J. Atmos. Sci., **21**, 634-639.

Clough, S. A., and R. A. A. Franks, 1991: The evaporation of frontal and other stratiform precipitation. Quart. J. Roy. Meteor. Soc., 117, 1057–1080.

Diederich, M. and R. Evaristo, 2015: Four-Dimensional Merging of Polarimetric Weather Radar Scans in Germany at X and C Band Wavelenghts. Presentation at the AMS radar conference, Norman, Oklahoma.

Hlad, C. J., Jr., 1944: Stability-tendency and mammatocumulus clouds. Bull. Amer. Meteor. Soc., **25**, 327–331.

Martner, B. E., 1995: Doppler radar observations of mammatus. Mon. Wea. Rev., 123, 3115–3121.

Löhnert, U., J. H. Schween, C. Acquistapace, K. Ebell, M. Maahn, M. Barrera-Verdejo, A. Hirsikko, B. Bohn, A. Knaps, E. O'Connor, C. Simmer, A. Wahner, and S. Crewell, 2015: JOYCE: Jülich Observatory for Cloud Evolution. Bull. Amer. Meteor. *Soc.*, **96**, 1157–1174.

Martner, B. E., 1996: An intimate look at clouds. Weatherwise, **49(3)**, 20–23.

Picca, J. C., M. R. Kumjian, and A.V. Ryzhkov, 2010: Z_{DR} Columns as a predictive tool for hail groth and storm evolution. 25th Conf. on Severe Local Storms, Denver, CO, Amer. Meteo. Soc., Extended Abstracts, 11.3.

Rauber, R. M. and A. Tokay, 1991: An Explanation for the Existence of Supercooled Water at the Top of Cold Clouds. J. Atmos. Sci., **48**, 1005–1023.

Schultz, D. M., K. M. Kanak, J. M. Straka, R. J. Trapp, B. A. Gordon, D. S. Zrnić, G. H. Bryan, Adam J. Durant, Timothy J. Garrett, Petra M. Klein, and Douglas K. Lilly, 2006: The Mysteries of Mammatus Clouds: Observations and Formation Mechanisms. J. Atmos. Sci., **63**, 2409–2435.

Snyder, J., A. Ryzhkov, M. Kumjian, J. Picca, and A. Khain, 2015: Developing a Z_{DR} column detection algorithm to examine convective storm updrafts. Weather and Forecasting, in press.

Stith, J. L., 1995: In situ measurements and observations of cumulonimbus mamma. Mon. Wea. Rev., **123**, 907–914.